

Quantum Well Intermixing for Monolithic Integration: A Demonstration of Novel Widely-Tunable 10Gb/s Transmitters and Wavelength Converters

James W. Raring[†], Erik J. Skogen^{*}, Leif A. Johansson, Matt N. Sysak^{*}, Jonathon S. Barton[†],
Milan L. Masanovic^{*}, and Larry A. Coldren^{**†}

[†]Materials Dept. University of California, Santa Barbara, CA 93106

^{*}ECE Dept. University of California, Santa Barbara, CA 93106

Phone: 805.893.8465, Fax: 805.893.4500, Email: jraring@engineering.ucsb.edu

Abstract: Wavelength-agile InGaAsP/InP photonic integrated circuits were fabricated using a quantum well intermixing processing platform. 10Gb/s operation was achieved with widely-tunable laser/modulator transmitters and optoelectronic wavelength converters in the 1550 nm range.

©2004 Optical Society of America

OCIS codes: (140.5960) Semiconductor lasers; (140.3600) Lasers, tunable; (250.5300) Photonic Integrated Circuits

Quantum Well Intermixing for Monolithic Integration: A Demonstration of Novel Widely-Tunable 10Gb/s Transmitters and Wavelength Converters

James W. Raring[†], Erik J. Skogen^{*}, Leif A. Johansson, Matt Sysak^{*}, Jonathon S. Barton[†],
Milan L. Masanovic^{*}, and Larry A. Coldren^{**†}

^{*}Materials Dept. University of California, Santa Barbara, CA 93106

[†]ECE Dept. University of California, Santa Barbara, CA 93106

Phone: 805.893.8465, Fax: 805.893.4500, Email: jraring@engineering.ucsb.edu

Abstract: Wavelength-agile InGaAsP/InP photonic integrated circuits were fabricated using a quantum well intermixing processing platform. 10Gb/s operation was achieved with widely-tunable laser/modulator transmitters and optoelectronic wavelength converters in the 1550 nm range.

©2004 Optical Society of America

OCIS codes: (140.5960) Semiconductor lasers; (140.3600) Lasers, tunable; (250.5300) Photonic Integrated Circuits

1. INTRODUCTION

Optical networks employing wavelength division multiplexing (WDM) will benefit tremendously by exploiting photonic integrated circuits (PICs) with wavelength-agile capabilities. Widely-tunable transmitters are the key to achieving cost savings through inventory reduction and are an enabling technology for future applications such as dynamic provisioning [1,2]. The integration of an optical receiver with a widely-tunable transmitter can provide wavelength conversion functionality, making applications such as wavelength routing and reconfigurable optical add/drop multiplexes (ROADMs) possible [3].

The capacity to fabricate such wavelength-agile PICs requires a processing platform ideal for the monolithic integration of components with differing functionality. These components inherently require a specific band edge for optimum performance. Quantum well intermixing (QWI) has been shown to provide device specific band edge definition orthogonal to the growth direction [4], with high controllability and resolution. The work presented herein utilizes QWI to realize a high performance wavelength-agile transmitter and wavelength conversion at 10Gb/s.

2. EXPERIMENT

The lithographic mask contains two variations of the photonic integrated circuit architecture, which are shown in Fig. 1. Both architectures consist of two adjacent parallel buried ridges, which can function independent of one another, with one ridge operating as an optical receiver and the adjacent ridge operating as an optical transmitter. The receiving ridge consists of a semiconductor optical amplifier (SOA) and a photo-detector for the amplification and detection of the input optical signal, respectively. The adjacent transmitting ridge consists of a four section widely tunable sampled-grating (SG) distributed Bragg reflector (DBR) laser followed by an electro-absorption

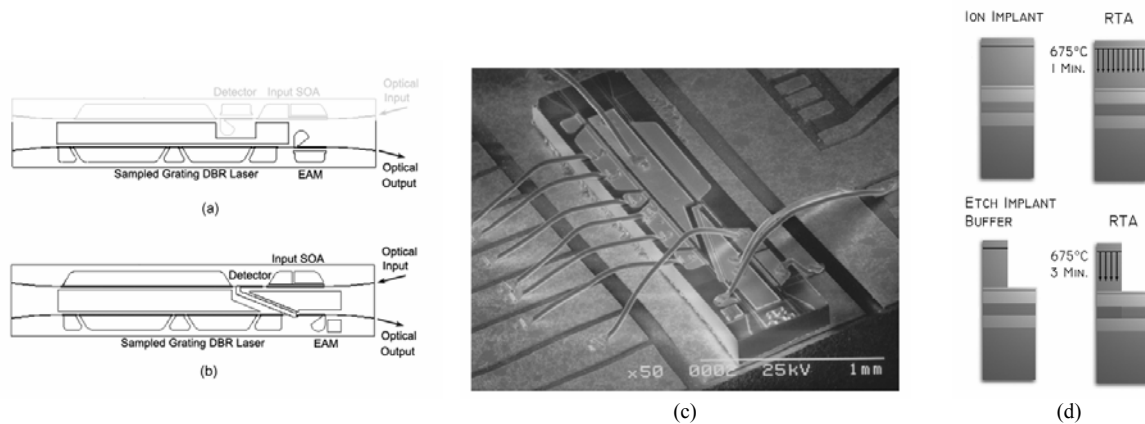


FIGURE 1. (a) Top view schematic of the device with discrete detector/modulator architecture, where the transmitter device used in this work is shown with dark outline. (b) Top view schematic of the interconnected device used in the wavelength converter work. (c) Electron micrograph of the completed wavelength converter device mounted on carrier (d) Illustration of the intermixing processing platform used in this work.

modulator (EAM). The 4 sections of the SG-DBR laser are: gain, back mirror, phase, and front mirror of which, the latter three function to tune the wavelength of the laser. The lone difference between the two architectures is the electrode scheme placed on the detector and EAM. In the first scheme, Fig 1a, the detector and EAM have discrete electrodes such that they can each be biased independently, allowing for the testing of the SG-DBR/EAM ridge solely as a transmitter. In the second architecture, termed the optoelectronic integrated circuit (OEIC) wavelength converter, the detector and EAM electrodes are joined by a CPS interconnect. In this configuration, the photocurrent generated in the detector by the input optical signal will pass through a termination load, resulting in the small signal voltage swing across the EAM identical to that of the input data sequence. The EAM functions to write the data on the continuous wave output of the SG-DBR laser operating at any wavelength within the tuning band hence wavelength conversion is achieved. A scanning electron micrograph of the second architecture is shown in Fig. 1c.

In this work, we employ a modified ion-implantation enhanced QWI process described in [1], as the fabrication platform for the realization of the described OEIC architectures. This method relies on the diffusion of point defects, specifically vacancies, created during an ion implantation. As the vacancies diffuse through the MQW active region during a high temperature anneal, group V atoms interdiffuse between the wells and barriers. This results in a more parabolic shaped well, increasing the quantized energy level separation between the conduction and valence bands, and hence blue shifting the band edge.

To achieve 10Gb/s operation, several measures were taken for the reduction of parasitic capacitance. The epilayer base structure was grown on a semi-insulating substrate, benzocyclobutene (BCB) was defined below the EAM electrodes to serve as a low-K dielectric, and an angled proton implant was performed adjacent to the buried ridge to eliminate the parasitic capacitance associated with the homojunction.

3. PROCESS

The epitaxial base structure contained an n-contact InGaAs layer 1 μm below a multi-quantum well (MQW) active region centered within a 1.1Q waveguide. The MQW consists of 15 InGaAsP 8.0 nm compressively strained (0.6%) quantum wells, separated by 8.0 nm tensile strained (0.3%) InGaAsP barriers grown on a Fe-doped InP substrate using a Thomas Swan horizontal-flow rotating-disc MOCVD reactor. Following the active region, a 15 nm InP stop etch, a 20 nm 1.3Q stop etch, and a 450 nm InP implant buffer layer was grown.

A 500 nm Si_xN_y mask layer was deposited using plasma enhanced chemical vapor deposition and lithographically patterned such that it remained only where the as-grown band-edge was desired. Ion implantation was performed using P^+ at an energy of 100 keV, yielding a range of 90 nm, with a dose of $5 \times 10^{14} \text{ cm}^{-2}$, at a substrate temperature of 200 $^\circ\text{C}$ [4]. The sample was subjected to rapid thermal processing at a temperature of 675 $^\circ\text{C}$, promoting the diffusion of vacancies through the MQW region. Once the desired band-edge for the EAM was achieved ($\lambda_{\text{pl}} = 1510 \text{ nm}$) the diffusion process was halted. The implant buffer layer above the EAM sections was removed using a wet etching process, stopping on the 1.3Q stop etch layer. The sample was then subjected to an additional rapid thermal anneal, further blue-shifting the regions where the implant buffer layer remained. This second anneal was used to obtain desired band edge ($\lambda_{\text{pl}} = 1450 \text{ nm}$) for the mirror, phase, and passive waveguide sections. A schematic illustrating the intermixing process and the photoluminescence of the active, EAM, and passive regions are shown in Fig. 1d and 2a, respectively.

The remainder of the process was carried out as described in [1] with the modifications for top-side n-contacts and the addition of BCB beneath the EAM contacts. The wafers were thinned, the devices were cleaved into bars

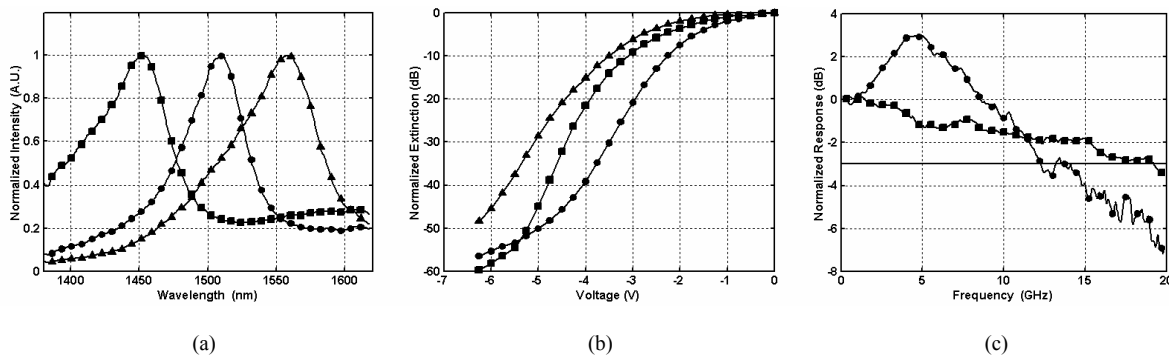
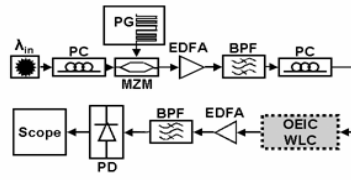
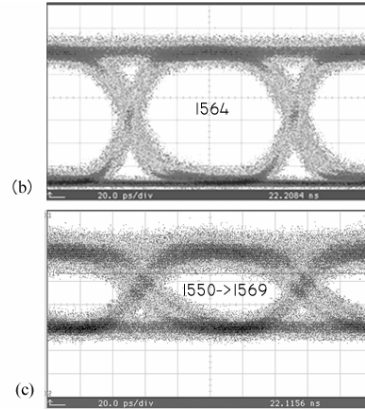


FIGURE 2. (a) Photoluminescence spectra of active section (triangles), modulator section (circles), and passive sections (squares). (b) DC extinction of a 175 μm modulator for wavelengths of 1558 nm (circles), 1570 nm (squares), and 1580 nm (triangles). (c) Electrical to optical frequency response of the transmitter device (squares) and optical to optical frequency response for wavelength converter device.



PC- Polarization Controller
 PG- Pattern Generator
 MZM- LiNbO₃ Mach-Zehnder Modulator
 EDFA- Erbium Doped Fiber Amplifier
 BPF- Band Pass Filter
 WLC- Wavelength Converter
 PD- Photodiode Receiver
 Scope- Oscilloscope

(a)



(b)

(c)

FIGURE 3. (a) Test set used to measure the eye diagrams for the wavelength converter device. (b) 10 Gb/s transmitter device representative eye diagram at 1564 nm (c) 10 Gb/s representative eye diagrams for wavelength conversion from 1550 nm to 1569 nm.

and anti-reflection coated. The die were separated, soldered to aluminum nitride carriers, and wire bonded (Fig. 1c) for characterization.

4. RESULTS

The SG-DBR lasers demonstrated low threshold currents of around 13mA, with output powers of 10mW at a gain section current of 100mA, with a side mode suppression ratio (SMSR) greater than 35 dB. The DC modal extinction characteristics of a 175 μm long EAM are presented in Fig. 2b. Over 40 dB of extinction was demonstrated for wavelengths of 1558, 1570, and 1580 nm, with efficiencies greater than 20dB/Volt. The 3dB bandwidth of the same modulator was greater than 19 GHz as shown in Fig. 2c. The optical to optical frequency response of a wavelength converter with a 225 μm photo-detector interconnected to a 175 μm modulator demonstrated a 3dB bandwidth of over 12 GHz, also shown in Fig. 2c. The resonance in the response at lower frequencies of this device is believed to be caused by inductance in the wire bond from the modulator to the RF pad on the carrier.

To demonstrate operation of both wavelength conversion and transmission at 10Gb/s, eye diagrams were taken for each type of device and bit error rate (BER) testing was performed through various fiber lengths for the SG-DBR/EAM transmitters. The test scheme used to obtain eye diagrams from the wavelength converter is shown Fig. 3a. The scheme used to obtain eye diagrams from the transmitter differs from the scheme in Fig. 3a such that electrically amplified data from the pattern generator was supplied to the device. Eye diagrams from the transmitter device and wavelength converter device, demonstrating conversion from 1550 nm to 1569 nm, are shown in Fig. 3b and 3c, respectively. Greater than 10 dB extinction was realized at wavelengths of 1558, 1564, and 1571 nm from the transmitter device, and error-free operation was achieved through 75km of fiber, with a power penalty of less than 0.5 dB. Error-free operation was achieved for conversion from 1550 to 1561, with a power penalty of 8dB. The high power penalty is a result of insufficient extinction (2 dB) due to the poor efficiency of the receiver.

5. CONCLUSION

A QWI processing platform has been employed for the fabrication of wavelength-agile photonic integrated circuits. Both discrete SG-DBR/EAM transmitters and OEIC wavelength converters have been confirmed at 10 Gb/s. The transmitters demonstrated a 3dB bandwidth over 19 GHz, an RF extinction greater than 10 dB, and error-free transmission through 75 km of non-dispersion shifted fiber with a minimal power penalty. The concept of OEIC wavelength conversion at 10 Gb/s has been realized. Significant improvements in the receiver design will yield increased RF extinction, reducing the power penalty of conversion.

6. REFERENCES

- [1] E. Skogen, J. Raring, J. Barton, S. DenBaars, and L. Coldren, "Post-Growth Control of the Quantum-Well Band Edge for the Monolithic Integration of Widely-Tunable Lasers and Electroabsorption Modulators," *IEEE J. Sel. Topics Quantum Electron.* To be published 2004.
- [2] J. Barton, M. Mašanovic, E. Skogen, and L. Coldren, "Widely-Tunable High-Speed Transmitters Using Integrated SGDBRs and Mach-Zehnder Modulators," Accepted for publication in *J. Sel. Topics in Quantum Electron.*, vol. 9, September/October, 2003.
- [3] M. Mašanovic, V. Lal, J. Barton, E. Skogen, L. Coldren, and D. Blumenthal, "Monolithically Integrated Mach-Zehnder Interferometer Wavelength Converter and Widely-tunable Laser in InP," *IEEE Photon. Technol. Lett.*, vol. 15, pp.1117-1119, 2003.
- [4] E. Skogen, J. Barton, S. DenBaars, and L. Coldren, "Tunable Sampled-Grating DBR Lasers Using Quantum-Well-Intermixing," *IEEE Photon. Technol. Lett.*, vol. 14, pp.1243-5, 2002.